Infection, Genetics and Evolution 75 (2019) 103945

Contents lists available at ScienceDirect

Infection, Genetics and Evolution

journal homepage: www.elsevier.com/locate/meegid

Research paper

Analysis of the microRNA expression profiles in feline kidney cell line infected with feline panleukopenia virus

Lingling Zhang[a,b], Ruiying Liang[a,b], Guangzhi Zhang[a,b], Zhian Zhai[a,b], Yong Deng[d], Jinxiang Li[a,c,*], Shangjin Cui[a,b,**]

[a] Institute of Animal Sciences, Chinese Academy of Agricultural Sciences, Beijing 100193, China
[b] Scientific Observation and Experiment Station of Veterinary Drugs and Diagnostic Technology of Beijing, Ministry of Agriculture, Beijing 100193, China
[c] Chinese Academy of Agricultural Sciences, Beijing 100081, China
[d] China Institute of Veterinary Drug Control, Beijing 100081, China

ARTICLE INFO

The miRNAs profile raw data from this article have been deposited with the GEO under Accession No. as follows: GSM3465571, Ctrl-1; GSM3465572, Ctrl-2; GSM3465573, Ctrl-3; GSM3465574, FPV-1; GSM3465575, FPV-2; GSM3465576, FPV-3.

Keywords:
Feline kidney cell line
microRNA
FPV
Deep sequencing

ABSTRACT

MicroRNAs (miRNAs) play crucial roles in post-transcriptional regulation of gene expression in many biological processes. Feline panleukopenia virus (FPV) is a highly infectious pathogen that can cause severe disease in pets, economically important animals and wildlife. In this study, miRNAs associated with FPV infection were identified using high-throughput sequencing. Our results showed that 673 known miRNAs and 278 novel miRNAs were identified and 57 significantly differential expression miRNAs were found post-FPV infection in feline kidney cell line. Stem-loop qRT-PCR was applied to validate the expression of the randomly selected miRNAs; the results were consistent with the sequencing data. Furthermore, the target genes of differential expression miRNAs were analyzed and predicated by GO and KEGG pathway. Altogether, our analysis provides a potential link between miRNA expression and the pathogenesis of FPV infection.

1. Introduction

MicroRNAs (miRNAs) are endogenous small non-coding RNAs with about 22 nucleotides in length that serve the pivotal function of regulating gene expression (Ambros, 2004). Instead of being translated into proteins (Crick, 1970), the mature single-stranded miRNA binds to messenger RNAs (mRNAs) to interfere with the translational process. They can affect many cellular functions, such as cell proliferation, hematopoiesis and development of the nervous system (Bartel, 2009; Yates et al., 2013). The first report on miRNA was presented in 1993 by Ambros and colleagues who described a 22-nucleotide RNA encoded by the lin-4 gene in *Caenorhabditis elegans*, which can bind to the lin-14 transcript and interfere with its expression (Lee et al., 1993). Several miRNAs have been identified in animals and plants since these seminal discoveries (Sun et al., 2010). Recently, miRNAs have been implicated in the intricate cross-talk between the host and the pathogen during viral infection and are thought to play a major role in viral pathogenesis (Nair and Zavolan, 2006). miRNAs can execute their gene regulation functions via multiple ways. Firstly, virus can exploit the miRNA system to facilitate its replication (Xie et al., 2018; Zhang et al., 2016). Secondly, multiple miRNAs in hosts have been identified as inhibitors of viral replications by directly targeting viral genomes or inhibiting factors necessary for viral life cycles (Zhang et al., 2014). Although the researches of miRNA-mediated host-virus interaction has greatly con tributed to a better understanding of the mechanism of virus infection and host counteraction, miRNAs functions involved in host-virus interactions still await more studies.

Feline Panleukopenia Virus (FPV) is one of the most important viral pathogens in pets, economically important animals and wildlife. FPV infection can cause an acute, highly contagious and fatal infectious disease, termed as Feline Panleukopenia. FPV is a small (18–25 nm) negative-sense single stranded DNA virus with a genome of about 5 kb (Decaro et al., 2008), and this virus has the widest host range and highest pathogenicity in the carnivore parvovirus subgroup. Its genome is comprised mainly of two open reading frames that express the non-structural proteins NS1 and NS2 and capsid proteins VP1 and VP2. FPV replicate using the host cell polymerases and other DNA replication machinery, which enables the virus to infect the rapidly dividing cells (Truyen and Parrish, 2013; Poncelet et al., 2016). FPV infection results in a high rate of morbidity and mortality with rapid clinical course and

* Correspondence to: J. Li, Chinese Academy of Agricultural Sciences, Beijing 100193, China.
** Correspondence to: S. Cui, Institute of Animal Science, Chinese Academy of Agricultural Sciences, Beijing 100193, China.
E-mail addresses: lijinxiang@caas.cn (J. Li), cuishangjin@caas.cn (S. Cui).

https://doi.org/10.1016/j.meegid.2019.103945
Received 14 March 2019; Received in revised form 23 June 2019; Accepted 28 June 2019
Available online 29 June 2019
1567-1348/

Table 1
Primer sequences used in stem-loop qRT-PCR of candidate miRNAs.

miRNAs	Stem-loop primers sequences (5′-3′)	RT-PCR forward primers sequences (5′-3′)
hsa-miR-22-3p	GTCGTATCCAGTGCAGGGTCCGAGGTATTCGCACTGGATACGACACAGTT	GCGAAGCTGCCAGTTGAAG
hsa-miR-15b-5p	GTCGTATCCAGTGCAGGGTCCGAGGTATTCGCACTGGATACGACTGTAAA	CGCGTAGCAGCACATCATGG
hsa-miR-574-3p	GTCGTATCCAGTGCAGGGTCCGAGGTATTCGCACTGGATACGACTGTGGG	CGCACGCTCATGCACACA
hsa-miR-106b-5p	GTCGTATCCAGTGCAGGGTCCGAGGTATTCGCACTGGATACGACATCTGC	GCGCGTAAAGTGCTGACAGT
hsa-miR-98-5p	GTCGTATCCAGTGCAGGGTCCGAGGTATTCGCACTGGATACGACAACAAT	CGCGCGTGAGGTAGTAAGTTGT
hsa-miR-146a-5p	GTCGTATCCAGTGCAGGGTCCGAGGTATTCGCACTGGATACGACAACCCA	CGCGTGAGAACTGAATTCCA
hsa-miR-197-3p	GTCGTATCCAGTGCAGGGTCCGAGGTATTCGCACTGGATACGACGCTGGG	GCGTTCACCACCTTCTCCA
hsa-miR-26a-1-3p	GTCGTATCCAGTGCAGGGTCCGAGGTATTCGCACTGGATACGACCGTGCA	GCGCGCCTATTCTTGGTTACT
hsa-miR-23b-5p_L-1	GTCGTATCCAGTGCAGGGTCCGAGGTATTCGCACTGGATACGACAAATCA	CGGGGTTCCTGGCATGC
pal-miR-9226-5p_L-4_1ss15GA	GTCGTATCCAGTGCAGGGTCCGAGGTATTCGCACTGGATACGACTGGCGC	GCGCGGTCCCTGTTCAG
hsa-miR-16-1-3p_R1	GTCGTATCCAGTGCAGGGTCCGAGGTATTCGCACTGGATACGACTTCAGC	CGCGCCAGTATTAACTGTGCT
sha-mir-24-1-p5_1ss2GC	GTCGTATCCAGTGCAGGGTCCGAGGTATTCGCACTGGATACGACCGGAGG	GCGTCGATTGGACCCGC
hsa-miR-92a-1-5p	GTCGTATCCAGTGCAGGGTCCGAGGTATTCGCACTGGATACGACAGCATT	GAGGTTGGGATCGGTTGC
hsa-miR-26a-2-3p	GTCGTATCCAGTGCAGGGTCCGAGGTATTCGCACTGGATACGACGAAACA	GCGCGCCTATTCTTGATTACT
hsa-miR-99b-5p	GTCGTATCCAGTGCAGGGTCCGAGGTATTCGCACTGGATACGACCGCAAG	CGCACCCGTAGAACCGAC

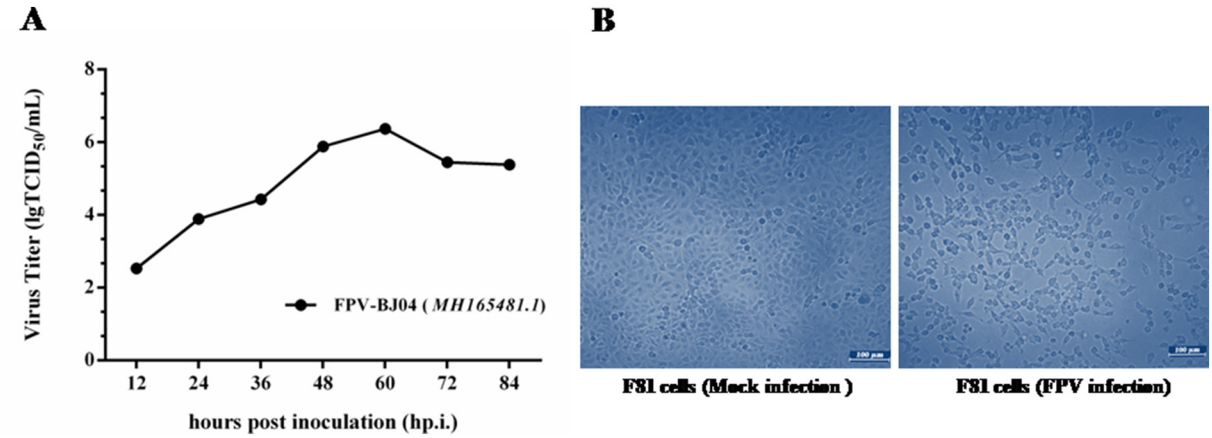

Fig. 1. Illustrates FPV growth curves in infected F81 cells. (A) Viral growth curves in F81 cells. FPV culture supernatants were diluted by 10-fold serial dilution method and viral titer was calculated by standard $TCID_{50}$ assay. (B) CPE of virus on F81cells were observed by bright-field microscopy after 48 h pi. Mock infection: F81 cells without FPV infection served as the negative control. FPV infection: Morphological changes in F81 cells when infected with FPV.

spread. In recently years, FPV has been epidemic in pets, economically important animals, and wildlife in China. Therefore, strategies to control FPV infection are required urgently to reduce the substantial losses caused by this viral disease. Currently, some studies about FPV have been reported on how to facilitate its replication (Kang et al., 2017). Meanwhile, the development of deep-sequencing technology is quite propitious to further explore the various roles of miRNAs in the immune defense against pathogenic infection.

Little attention has been paid until now to use domestic cat (*Felis catus*) as an experimental animal or a source of cell cultures. In this study, we summarized the first characterization and investigation of the miRNA expression profiles in the F81 cells under FPV infected or uninfected conditions using the Illumina's ultrahigh approach. Collectively, the integrated analysis of miRNAs from our research could provide more insight into the mechanism of miRNAs-mediated regulation of FPV.

2. Materials and methods

2.1. Cells and virus

FPV strain (FPV-BJ04, *MH165481.1*) originally isolated from feces of infected cats in a pet hospital in Beijing, China. Initially, the full genome of this strain has been sequenced accurately by our laboratory. F81 cells were obtained from the Cell Resource Center of the Shanghai Institute for Biological Science, Chinese Academy of Science, and maintained in Dulbecco's Modified Eagle Medium (DMEM) (Gibco, CA) containing 5% fetal bovine serum and 1% penicillin-streptomycin at 37 °C with 5% CO2.

2.2. FPV infection and viral one-step growth kinetics

FPV-free F81 cells were seeded into 96-well microtiter plates with 5% fetal bovine serum (FBS, Gibco) and were maintained in a humidified 5% CO_2 atmosphere for 12 h. After 80% confluence, the F81 cells were infected with 10-fold serial dilution of FPV-BJ04 virus stocks ($1:10^{-1}$ to $1:10^{-8}$). The cultures were observed for cytopathic effects (CPE) at different time intervals up to 84 h post infections (hp.i.). Viruses were quantified by already described method of Reed and Muench. Briefly, standard $TCID_{50}$ assay technique was used to calculate viral titer and subsequent quantification (Reed and Muench, 1938).

For construction of small RNA libraries, F81 cells were cultured in six-well-plates (Corning, USA) and divided into two groups, each group was performed three replicates. The first group was infected with FPV-BJ04 at a dose of 1×10^6 $TCID_{50}$, and the second group serves as uninfected control. At 48 h post-infection, FPV-BJ04 infected (FPV group) and uninfected cells (Ctrl group) were treated using Trizol reagent (Invitrogen, CA, USA) for the following total RNA extraction.

2.3. Construction of small RNA library and deep sequencing

For six small RNA library constructions, total RNAs were extracted from FPV group and Ctrl group using Trizol reagent (Invitrogen, CA, USA) following the manufacturer's instruction. The quantity and purity

Fig. 2. Small RNA reads from Ctrl group (FPV-uninfected) and FPV group (FPV-infected) were blasted against the Rfam database non-coding RNA to annotate rRNA, tRNA, snoRNA, snRNA and others RNAs.

Table 2
Overview of reads from raw data to cleaned sequences of small RNA sequences.

Type	Ctrl_1		Ctrl_2		Ctrl_3		FPV_1		FPV_2		FPV_3	
	Total	%	Total	%	Total	%	Total	%	Total	%	Total	%
Raw reads	12,868,828	100.00	10,655,668	100.00	10,628,208	100.00	14,279,121	100.00	10,141,913	100.00	10,545,204	100.00
3ADT&length filter	2,586,042	20.10	2,514,875	23.60	2,625,966	24.71	4,817,794	33.74	2,320,545	22.88	3,899,551	36.98
Junk reads	15,336	0.12	12,365	0.12	10,107	0.10	42,614	0.30	34,293	0.34	30,036	0.28
Rfam	2,529,089	19.65	1,664,630	15.62	1,835,996	17.27	2,245,062	15.72	1,760,691	17.36	1,621,185	15.37
Repeats	681,653	5.30	419,258	3.93	490,241	4.61	378,583	2.65	298,668	2.94	273,580	2.59
valid reads	5,828,402	45.29	4,877,852	45.78	4,640,929	43.67	5,414,083	37.92	4,538,421	44.75	3,827,415	36.30

Ctrl: FPV uninfected groups; FPV: FPV infected groups.

of each RNA sample was analysis using a Bioanalyzer 2100 with RIN number > 7.0 and RNA 6000 Nano LabChip Kit (Aglient, Santa Clara, CA, USA) with 28S/18S ratio between 1.8 and 2.2. Approximately 1 μg of total RNA was used to prepare small RNA library according to the protocol of TruSeq Small RNA Sample Prep Kits (Illumina, San Diego, USA) and the sRNA data was sequenced by Illumina Hiseq 2500 platform at the LC-BIO (Hangzhou, China) following the vendor's recommended protocol.

2.4. Small RNA bioinformatics analysis

The raw sequencing reads were subjected to an in-house program, ACGT101-miR (LC Sciences, Houston, Texas, USA) to remove adapter dimers, junk and low complexity data and were blasted against the Rfam (http://rfam.xfam.org) database to remove mRNA, rRNA, tRNA, snRNA, snoRNA, other non-coding RNAs and repeat sequences. Subsequently, the unique reads with length in 18–26 nucleotide were

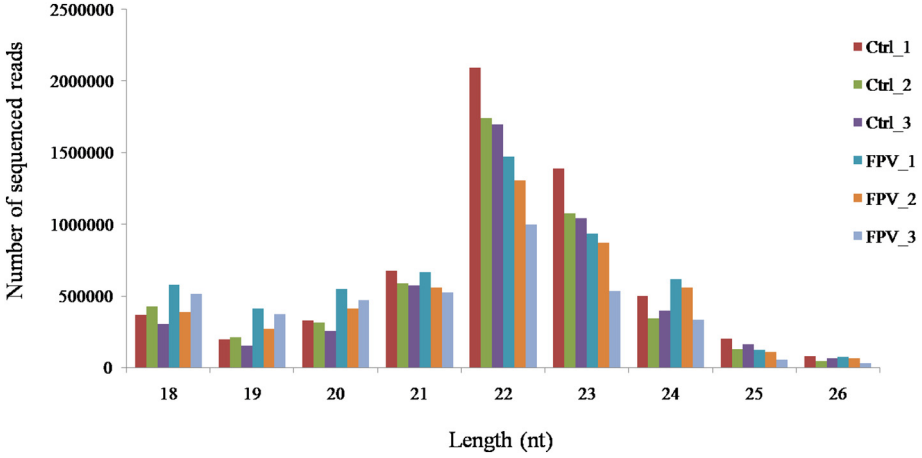

Fig. 3. Size distribution of sequenced small RNAs from Ctrl group and FPV group. The majority of the reads was 22 nt in length.

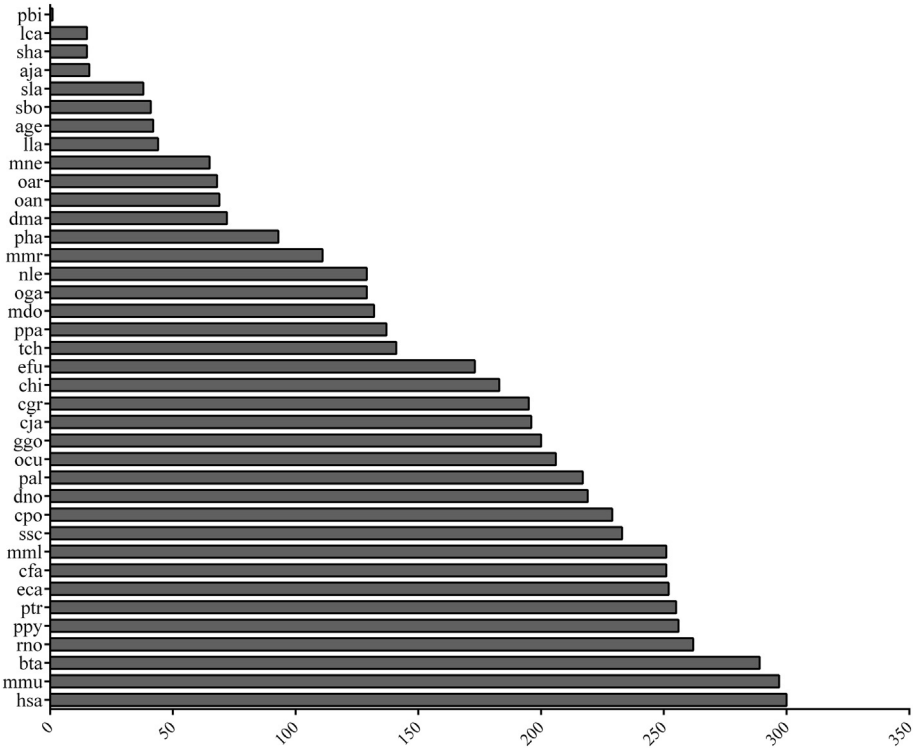

Fig. 4. Conservation profiles of identified miRNAs, values on the x-axis representing the number of known miRNAs compared to the corresponding species.

then mapped to miRBase 22.0 (http://www.mirbase.org/cgi-bin/browse.pl) by BLAST to identify known miRNAs and novel 3p- and 5p-derived miRNAs. Novel candidate miRNAs were identified by prediction of their secondary structures using Mfold program (http://unafold.rna.albany.edu/?q=mfold/RNA-Folding-Form).

2.5. Differential expression analysis of miRNAs

To compare the miRNA expression levels in six libraries to identify differentially expressed miRNAs, miRNA expression levels in each library was normalized as transcripts per million. Normalized expression (NE) = actual miRNA count/total count of clean reads. Differential expression of miRNAs based on normalized deep-sequencing counts was analyzed by selectively using Fisher exact-test, Chi-squared 2×2 test, Student *t*-test, or ANOVA based on the experimental design. The significance threshold was set to be 0.01 in each test.

2.6. The prediction of target genes of miRNAs

To predict the genes targeted by miRNAs, two computational target prediction algorithms (TargetScan 50: http://www.targetscan.org/) and (miRanda: http://www.microrna.org/microrna/home.do) were used to identify miRNA binding sites. Finally, the data predicted by both algorithms were combined and the overlaps were calculated. The GO terms (http://geneontology.org) and KEGG Pathway (http://www.genome.jp/kegg/) of these miRNAs and miRNA targets were also annotated.

2.7. Confirmation of miRNAs expression by stem-loop qRT-PCR

The infection methods were same as Section 2.1 and total RNAs of these samples were extracted as described above. We designed stem-loop primers as well as RT-PCR forward primers of 15 candidate miRNAs and the reverse primer: AGTGCAGGGTCCGAGGTATT

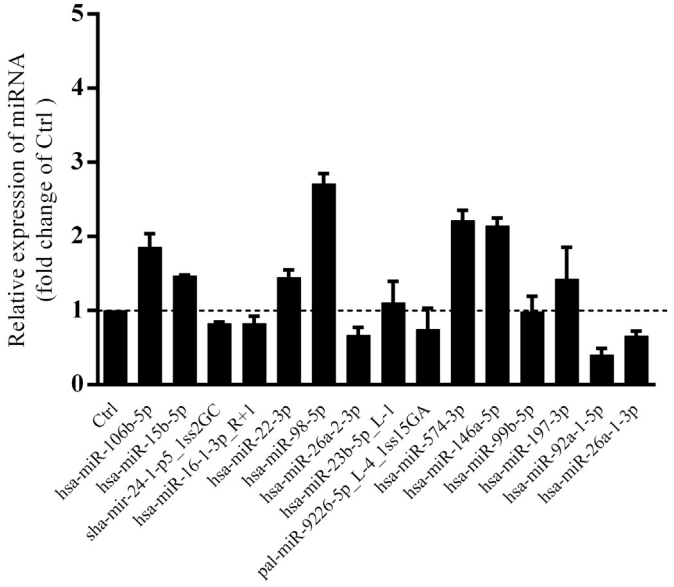

Fig. 5. Validation of relative expression of 15 randomly selected miRNAs by Stem-loop qRT-PCR in Ctrl and FPV group. Data were performed in triplicate, and the fold change of gene expression level was calculated based on U6 endogenous normalization.

matching with stem-loop primer. The miRNA 1st Strand cDNA Synthesis Kit and miRNA Universal SYBR® qPCR Master Mix (Vazyme, China) was used to quantify these mature miRNAs according to the manufacturer's instruction. 500 ng of total RNAs were used for cDNA synthesis and U6 RNA was used as an internal standard (U6F: CTCGC TTCGGCAGCACA; U6 R: AACGCTTCACGAATTTGCGT). All reactions were performed in triplicate on the CFX96 Real-time PCR Detection System (Bio-Rad, Hercules, CA, USA). $2^{-\Delta\Delta Ct}$ method was adopted to analyze the relative expression of the randomly selected miRNAs. All primers for stem-loop qRT-PCR are listed in Table 1.

3. Results

3.1. Virus growth and F81 cells cytopathic effects

One-step growth curve of the FPV showed that virus began to proliferate after 12 h infection and reached its maximum proliferation and growth after 60 h, and then stabilized. The cytopathic effects (CPE) were observable (Fig. 1B), at 48 h (as FPV was in proliferative phase at this stage, Fig. 1A).

3.2. Overview of the deep-sequencing data

Recently, some reports have indicated that parvovirus infection can cause the alterations of miRNAs expression in host cells (Sun et al., 2014; Li et al., 2015). However, the role of miRNAs in response to the FPV infection has not been reported.

To identify the miRNAs involved both FPV group and Ctrl group, sRNA libraries from these samples were sequenced side by side using the Illumina Hiseq 2500 platform. A total of 12,868,828; 10,655,668; 10,628,208 raw reads and 14,279,121; 10,141,913; 10,545,204 raw reads were processing in the Ctrl and FPV groups, respectively. After discarding junk sequences, sequences length > 27 nt or < 17 nt, RNA family (Rfam) sequences (rRNA, tRNA, snRNA, snoRNA and other Rfam RNAs) (Fig. 2) and repeat sequences, 5,828,402; 4,877,852; 4,640,929 and 5,414,083; 4,538,421; 3,827,415 high quality reads remained for further analysis (Table 2). Based on the criterion of filtering read length, we analyzed the length distribution and found that most of reads (71.37%) were distributed between 21 and 23 nt with 22 nt being the most abundant (Fig. 3). Our observations are consistent with many reports in other species (Huang et al., 2017; Strozzi et al., 2009; Hong et al., 2016).

3.3. Identification of conserved and novel miRNAs

To identify the miRNAs in the feline, the clean reads of each library were mapped to the known mature animal miRNAs deposited in miRBase 22.0. After Blastn searches and further analysis, 673 known miRNAs (Table S1) covering 210 miRNA families were identified (Table S2). The largest family was let-7 with 24 members, and Let-7 is a big miRNA family which is also highly conserved in metazoans from worm to humans (Roush and Slack, 2008). Previous studies suggest that that let-7 family miRNAs are important regulators of fundamental biological processes (Powers et al., 2016). The mir-10 (18 members) and mir-154 (16 members) were second and third largest miRNA families, respectively. Of the remaining miRNA families, 66 families only contained a single member. In our study, the conserved miRNAs was observed in comparison with 38 animal species (Fig. 4) with the most miRNA members being homologous to sequences from *Homo sapiens* (300), *Mus musculus* (297), *Bos Taurus* (289) and only one member was identified in *Pygathrix bieti*, respectively. This suggested the conservatism of mature miRNAs among organisms.

Sequencing reads that did not map to any of the known miRNAs were further analyzed to identify a great number of novel miRNAs. This analysis showed a total 278 novel miRNAs were identified from the two libraries altogether as having the typical miRNA stem-loop secondary structure. Among these novel miRNAs, there are 81 miRNAs present in all two libraries. These novel miRNAs had expression levels represented by from 1.67-4718 raw reads (Table S3). As demonstrated by previous studies, known miRNAs are often the high abundantly expressed miRNAs, while most novel miRNAs are among the least abundant (Berezikov et al., 2006). Consistent with previous studies, most of novel miRNAs found in this study were expressed at low reads (< 1000). We annotated the novel miRNAs sequences as PC-3p/PC-5p. The lengths of pre-miRNA sequences ranged from 55 to 159 nt. The G + C contents of these novel miRNAs ranged from 20.5% to 91.8%, with an average of 45.3%. The minimum free energy (MFE) ranged from −115.70 to −15.10 kcal/mol, with an average of −35.87, which accords with the characteristics of miRNA.

3.4. Validation of identified miRNAs by stem-loop qRT-PCR

Validating and quantifying the differentially expressed miRNAs in two libraries are important and useful to further understand the fundamental functions of these miRNAs (Lee et al., 2008). In our study, fifteen miRNAs were randomly selected for stem-loop qRT-PCR analysis in FPV infected cells and uninfected cells. Our results showed that the majority (14/15) of the randomly selected miRNAs expression by qRT-PCR were consistent with those obtained by deep sequencing (Fig. 5).

3.5. Target prediction and enrichment analysis of differential expression miRNAs

To better understand the physiological functions of differential expression miRNAs and it is necessary to identify their target genes. Target gene prediction was performed using TargetScan and miRanda. Among these 57 differential expression miRNAs (54 known miRNAs and 3 novel miRNAs) (Fig. 6 and Table S4), we obtained 123,301 target genes for known miRNAs and 9273 target genes for novel miRNAs, respectively (Table S5). Not surprisingly, one miRNA can regulates distinct genes, and multiple miRNAs can regulate a single gene, suggesting that the miRNA gene regulation network might be extremely complicated. Of course, these predicted target genes can provide valuable information for investigating the specific biological processes in FPV-host interaction.

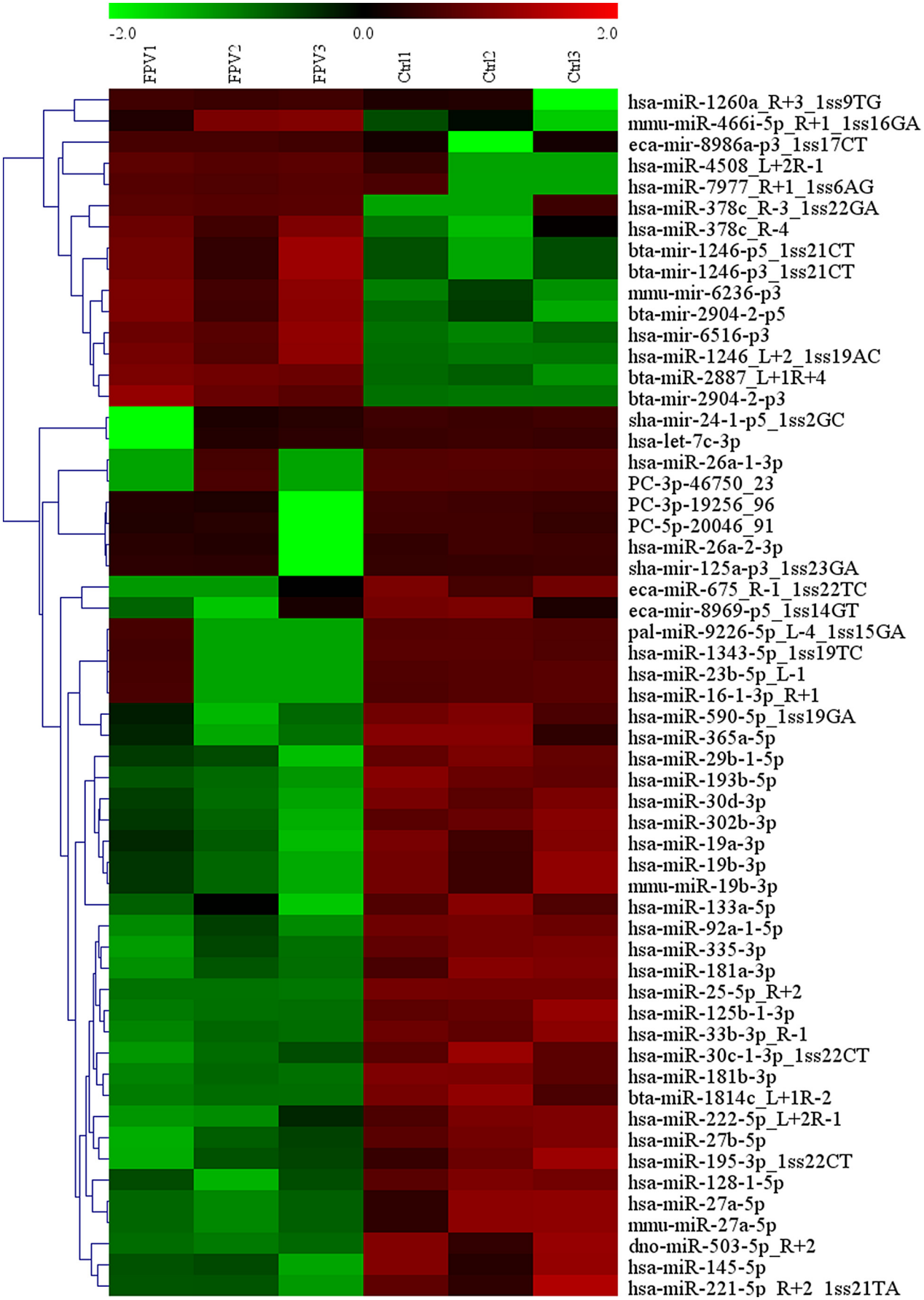

Fig. 6. Heat map showing the expression of differentially expressed miRNAs. The bar indicates relative expression level from high (red) to low (green). (For interpretation of the references to colour in this figure legend, the reader is referred to the web version of this article.)

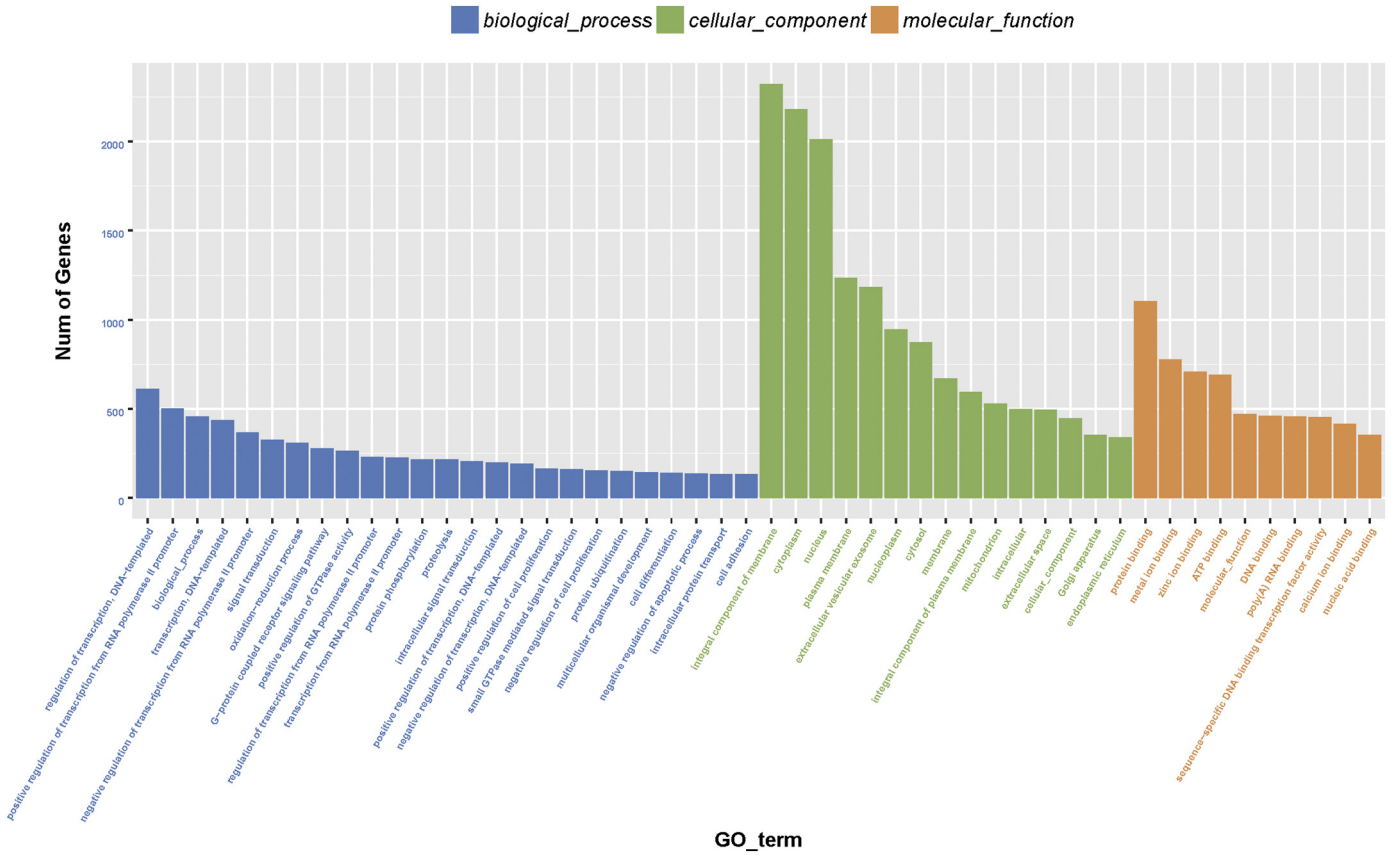

Fig. 7. Functional classification of differential expression miRNA s target genes according to GO category.

In order to better understand the physiological functions of predicated target genes of known and novel miRNAs, these target genes were subjected to GO analysis. GO analysis consists of three ontologies: biological process, molecular function and cellular component (Ashburner et al., 2000). The results revealed that 63,672, 34,341 and 38,874 genes classified into three category including 7861 biological process, 2874 molecular function and 1190 cellular component, respectively (Table 6S). As shown in Fig. 7, 25 categories in biological process were classified by annotated target genes, and a large numbers of targets are categorized as regulation of transcription DNA-templated, positive regulation of transcription from RNA polymerase II promoter and other biological process. In molecular function category, protein binding was the most significant enriched part with respect to 10 categories, followed by metal ion binding and zinc ion binding. The cellular component of GO term showed target genes were classified into 15 categories, of which they were enriched in integral component of membrane, cytoplasm and nucleus. It follows that the enrichment of each GO term is different within three ontologies. Notably, there were some high frequencies biological processes were enriched in cellular and metabolic processes.

In organisms, different genes perform their biological functions in coordination with each other. Pathway analysis based on KEGG database is helpful to further understand the biological functions of genes. In this study, KEGG analysis revealed that a total of 314 highly diversified pathway networks were involved with differential expression miRNAs target gene (Table 7S). As shown in Fig. 8, the top 20 most significantly enriched pathways are discovered to be involved in 6395 target genes. Most of target genes in these pathways were found to be involved in MAPK signaling pathway with 665 genes, followed by Focal adhesion (629 genes) and Regulation of actin cytoskeleton (609 genes). These results suggested that those potential targets might regulate the growth and development of Feline cells. Feline panleukopenia caused by FPV infection remains one of the most important infectious diseases for cats globally. It manifests primarily through profound anemia resulting in a significant decrease in the number of white blood cells. Based on the KEGG pathway and the clinical symptoms induced by FPV, we speculate that these potential target genes which are regulated by corresponding miRNAs may play a key role in the obvious symptoms of leucopenia. Further identification of the target genes of these miRNAs could shed new light on their regulatory roles of miRNAs in the interaction between FPV and host.

4. Conclusion

Present study was carried out in F81 cell line with or without FPV infection to analyze functions of miRNAs. In this experiment six small RNA libraries were successfully constructed through deep sequencing. A total of 673 known miRNAs and 278 novel miRNAs were identified, among which, 54 known and 3 novel miRNAs were differential expression miRNAs. The data from Stem-loop qRT-PCR analysis confirmed that randomly selected (15) most (14) miRNAs were expressed in F81 cells, which were consistent with data from deep sequencing. Further evaluation of target genes by GO and KEGG enrichment methods for differential expression of miRNAs reveal that these miRNAs play important roles in the multiple physiological processes.

Most importantly the data and results of present study provide a significant number of valuable novel miRNAs to the current database and provide novel insight into the molecular mechanism of FPV-host interaction and vaccine development.

Declaration of Competing Interest

The authors declare no conflict of interest.

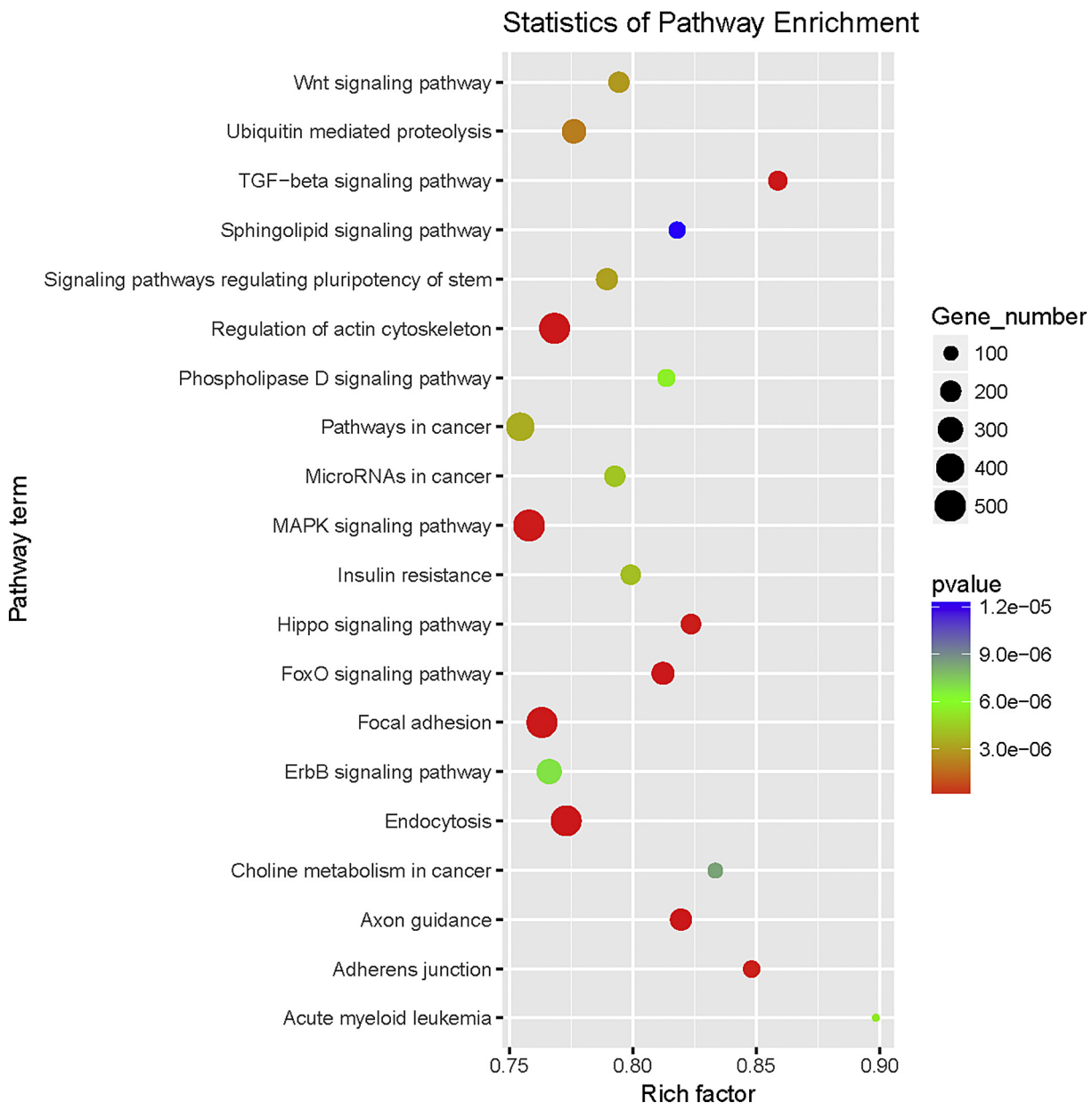

Fig. 8. KEGG pathways enriched analysis for target genes of differentially expressed miRNAs.

Acknowledgments

This work was supported by the Agricultural Science and Technology Innovation Program (ASTIP-IAS15), National Natural Science Foundation of China (NO.31172349 & NO.31172341) and the National Key Research and Development Program of China (No.2016YFD0501003 & 2017YFD0502300).

Appendix A. Supplementary data

Supplementary data to this article can be found online at https://doi.org/10.1016/j.meegid.2019.103945.

References

Ambros, V., 2004. The functions of animal microRNAs. Nature 431, 350–355.

Ashburner, M., Ball, C.A., Blake, J.A., Botstein, D., Butler, H., Cherry, J.M., Davis, A.P., Dolinski, K., Dwight, S.S., Eppig, J.T., Harris, M.A., Hill, D.P., Issel-Tarver, L., Kasarskis, A., Lewis, S., Matese, J.C., Richardson, J.E., Ringwald, M., Rubin, G.M., Sherlock, G., 2000. Gene ontology: tool for the unification of biology. Nat. Genet. 25, 25–29.

Bartel, D.P., 2009. MicroRNAs: target recognition and regulatory functions. Cell. 136, 215–233.

Berezikov, E., Thuemmler, F., van Laake, L.W., Kondova, I., Bontrop, R., Cuppen, E., Plasterk, R.H., 2006. Diversity of microRNAs in human and chimpanzee brain. Nat. Genet. 38, 1375–1377.

Crick, F., 1970. Central dogma of molecular biology. Nature. 227, 561–563.

Decaro, N., Desario, C., Miccolupo, A., Campolo, M., Parisi, A., Martella, V., Amorisco, F., Lucente, M.S., Lavazza, A., Buonavoglia, C., 2008. Genetic analysis of feline panleukopenia viruses from cats with gastroenteritis. J. Gen. Virol. 89, 2290–2298.

Hong, X., Qin, J., Chen, R., Yuan, L., Zha, J., Wang, Z., 2016. Identification and characterization of novel and conserved microRNAs in several tissues of the Chinese rare minnow (*Gobiocypris rarus*) based on illumine deep sequencing technology. BMC Genomics 17, 283.

Huang, Y., Gong, W., Ren, H., Xiong, J., Gao, X., Sun, X., 2017. Identification of the conserved and novel micreRNAs by deep sequencing and prediction of their targets in topmouth culter. Gene. 626, 298–304.

Kang, H.T., Liu, D.F., Tian, Jin., Hu, X.L., Zhang, X.Z., Yin, H., Wu, H.X., Liu, C.g., Guo, D.C., Li, Z.J., Jiang, Q., Liu, J.S., Qu, L.D., 2017. Feline panleucopenia virus NS2 suppresses the host IFN-β induction by disrupting the interaction between TBK1 and STING. Viruses. 9, 23.

Lee, R.C., Feinbaum, R.L., Ambros, V., 1993. The C. elegans heterochronic gene lin-4 encodes small RNAs with antisense complementarity to lin-14. Cell. 75, 843–854.

Lee, I., Ajay, S.S., Chen, H., Maruyama, A., Wang, N., McInnis, M.G., Athey, B.D., 2008.

Discriminating single-base difference miRNA expression using microarray Probe Design Guru (ProDeG). Nucleic Acids Res. 36, e27.
Li, X.Q., Zhu, L., Liu, X., Sun, X.G., Zhou, Y.C., Lang, Q.L., Li, P., Cai, Y.H., Qiao, X.G., Xu, Z.W., 2015. Differential expression of microRNAs in porcine parvovirus infected porcine cell line. Virol. J. 12, 128.
Nair, V., Zavolan, M., 2006. Virus-encoded microRNAs: novel regulators of gene expression. Trends Microbiol. 14, 169–175.
Poncelet, L., Garigliany, M., Ando, K., Franssen, M., Desmecht, D., Brion, J.P., 2016. Cell cycle S phase markers are expressed in cerebral neuron nuclei of cats infected by the feline panleukopenia virus. Cell Cycle 15, 3482–3489.
Powers, J.T., Tsanov, K.M., Pearson, D.S., Roels, F., Spina, C.S., Ebright, R., Seligson, M., Soysa, T.de., Cahan, P., Theissen, J., Tu, H.C., Han, A., Kurek, K.C., Lapier, G.S., Osborne, J.K., Ross, S.J., Cesana, M., Collins, J.J., Berthold, F., Daley, G.Q., 2016. Multiple mechanisms disrupt the let-7 microRNA family in neuroblastoma. Nature. 535, 246–251.
Reed, L.J., Muench, H., 1938. A simple method of estimating fifty percent endpoints. Am. J. Hygiene. 27, 493–497.
Roush, S., Slack, F.J., 2008. The let-7 family of microRNAs. Trends Cell Biol. 18, 505–516.
Strozzi, F., Mazza, R., Malinverni, R., Williams, J.L., 2009. Annotation of 390 bovine miRNA genes by sequence similarity with other species. Anim. Genet. 40, 125.
Sun, W., Julie Li, Y.S., Huang, H.D., Shyy, J.Y., Chien, S., 2010. MicroRNA: a master regulator of cellular processes for bioengineering systems. Annu. Rev. Biomed. Eng. 12, 1–27.
Sun, J.Z., Wang, J.G., Wang, S., Yuan, D.L., Birame, B.M., Li, Z.L., Yi, B., Liu, W.Q., 2014. MicroRNA profile analysis of a feline kidney cell line before and after infection with mink enteritis virus. Gene. 539, 224–229.
Truyen, U., Parrish, C.R., 2013. Feline panleukopenia virus: its interesting evolution and current problems in immunoprophylaxis against a serious pathogen. Vet. Microbiol. 165, 29–32.
Xie, Y.T., He, S.L., Wang, J.H., 2018. MicroRNA-373 facilitates HSV-1 replication through suppression of type I IFN response by targeting IRF1. Biomed. Pharmacother. 97, 1409–1416.
Yates, L.A., Norbury, C.J., Gilbert, R.C., 2013. The long and short of microRNA. Cell. 153, 516–519.
Zhang, Q., Guo, X.K., Gao, L., Huang, C., Li, N., Jia, X.J., Liu, W.J., Feng, W.H., 2014. MicroRNA-23 inhibits PRRSV replication by directly targeting PRRSV RNA and possibly by upregulating type I interferons. Virology. 450-451, 182–195.
Zhang, Q., Huang, C., Yang, Q., Gao, L., Liu, H.C., Tang, J., Feng, W.H., 2016. MicroRNA-30c modulates type I IFN responses to facilitate porcine reproductive and respiratory syndrome virus infection by targeting JAK1. J. Immunol. 196, 2272–2282.